

Dual-Flattening Transformers through Decomposed Row and Column Queries for Semantic Segmentation

Ying Wang¹ Chiuman Ho¹ Wenju Xu^{1,2} Ziwei Xuan^{*3} Xudong Liu¹
Guo-Jun Qi^{†1}

¹ OPPO US Research Center ² InnoPeak Technology, Inc. ³ Texas A&M University

{ying.wang, chiuman, wenju.xu, xudong.liu}@oppo.com, xuan64@tamu.edu, guojunq@gmail.com

Abstract

It is critical to obtain high resolution features with long range dependency for dense prediction tasks such as semantic segmentation. To generate high-resolution output of size $H \times W$ from a low-resolution feature map of size $h \times w$ ($hw \ll HW$), a naive dense transformer incurs an intractable complexity of $\mathcal{O}(hwHW)$, limiting its application on high-resolution dense prediction. We propose a Dual-Flattening Transformer (DFlatFormer) to enable high-resolution output by reducing complexity to $\mathcal{O}(hw(H + W))$ that is multiple orders of magnitude smaller than the naive dense transformer. Decomposed queries are presented to retrieve row and column attentions tractably through separate transformers, and their outputs are combined to form a dense feature map at high resolution. To this end, the input sequence fed from an encoder is row-wise and column-wise flattened to align with decomposed queries by preserving their row and column structures, respectively. Row and column transformers also interact with each other to capture their mutual attentions with the spatial crossings between rows and columns. We also propose to perform attentions through efficient grouping and pooling to further reduce the model complexity. Extensive experiments on ADE20K and Cityscapes datasets demonstrate the superiority of the proposed dual-flattening transformer architecture with higher mIoUs.

1. Introduction

Obtaining high-resolution features is important in many computer vision tasks, especially for dense prediction problems such as semantic segmentation, object detection and pose estimation. Typical approaches employ convolutional encoder-decoder architectures where the encoder outputs low-resolution features and decoder upsamples features with simple filters such as bilinear interpolation. Bi-

linear upsampling has limited capacity in obtaining high-resolution features, as it only conducts linear interpolation between neighboring pixels without considering non-linear dependencies in global contexts. Various approaches have been proposed to improve the high-resolution feature quality, such as PointRend [20] and DUpsample [28]. PointRend [20] carefully selects uncertain points in the downsampled feature space and refines them by incorporating low-level features. DUpsample [28] adopts a data-dependent upsampling strategy to recover segmentation from the coarse prediction. However, these approaches lack the ability in capturing long-range dependency for fine-grained details. Diverse non-local or self-attention based schemes have been proposed to enhance the output features [3, 17, 18, 31], but mostly in the downsampled feature space. They still rely on bilinear upsampling procedure to obtain high-resolution features which tends to lose global information.

Recently, transformers have drawn tremendous interests, due to its great success in capturing long-range dependency. As the first standard-alone transformer for computer vision, Vision Transformer (ViT) [13] shows impressive result on image classification with patch-based self-attentions. However there is still a large room to improve when applying to dense prediction tasks due to its low-resolution feature map caused by non-overlapping patches and intractable computing costs. The complexity of a naive dense transformer scales rapidly w.r.t the high-resolution output, limiting its application to dense prediction problems. Multi-scale ViTs [24, 33, 35, 37] have been presented to achieve hierarchical features with different resolutions and have boosted the performance of many dense prediction tasks. However, upper-level features with low spatial resolution still rely on bilinear upsampling to recover the full-resolution features. The naive bilinear upsampling is inherently weak since it is intrinsically linear and local in recovering fine-grained details by linearly interpolating from local neighbors.

Several efficient attention designs can reduce the model

*Work conducted during an internship at OPPO US Research Center.

†Corresponding author: Guo-Jun Qi, Email: guojunq@gmail.com.

complexity, such as Axial-attention [31], Criss-Cross attention [18] and LongFormer [2]. However, they mainly focus on feature enhancement in the downsampled space without recovering the high-resolution features or recovering the fine-grained details by modeling the nonlinear dependency on a more global scale from non-local neighbors. Therefore, in this paper, we strive to develop a transformer architecture that is not only efficient to recover full-resolution features but also able to recover the fine-grained details by exploring full contexts nonlinearly and globally.

For this purpose, to reduce the complexity w.r.t. to the high-resolution size, we propose a Dual-Flattening transformer (DFlatFormer) with decomposed row and column queries to capture global attentions. The key idea is to decompose the output feature space into row and column ones, and utilize the corresponding queries to output row and column representations separately. The final feature map can be obtained by integrating the two outputs. Let the size of a low-resolution input be $h \times w$, and the target high-resolution output size be $H \times W$. Our model only incurs a complexity of $\mathcal{O}(hw(H + W))$, while the naive dense transformer has a much larger complexity of $\mathcal{O}(hwHW)$ as $h \ll H$ and $w \ll W$. Our motivation is partially analogy to depth-wise separable convolution [8] which decomposes regular convolution into depth-wise and point-wise ones for reducing the complexity, whereas ours decompose a transformer into rows and columns before they interact with each other and are eventually re-coupled to form a dense feature map.

To accommodate with the decomposed row and column queries, we propose to flatten an input feature map row-wise and column-wise into two separate sequences, so that successive rows and columns are put together to preserve their row and column structures, respectively. This will enable row and column queries to retrieve their immediate contexts from the neighboring rows and columns. In this way, the dual-flattened sequences will ideally align with the query sequences of rows and columns, resulting in a dual-flattening transformer architecture presented in this paper.

With these dual-flattened sequences as input, the DFlatFormer employs a row and a column transformer, each generating row and column outputs at a higher resolution, respectively. Each transformer is composed of several layers of multi-head attentions between the decomposed queries and dual-flattened inputs followed by feed-forward networks (FFNs). Moreover, to refine the spatial details, we introduce row-column interactive attentions to reflect the crossing points between rows and columns. In this way, the sequences of row and column outputs will fully interact to share their learned representations in their vertical and horizontal contexts when they spatially cross each other. To further reduce the complexity, we apply grouping and pooling to query sequences and/or flattened inputs, enabling more efficient computing of attentions.

Our major contributions are summarized below.

- We propose an efficient dual-flattening transformer architecture to obtain high-resolution feature map, with a complexity of $\mathcal{O}(hw(H + W))$ where $h \times w$ and $H \times W$ are the input and output feature map sizes, respectively. The proposed architecture can serve as a flexible plug-in module into any CNN or transformer-based encoders to obtain high-resolution dense predictions.
- For this purpose, we propose to flatten input sequences row-wise and column-wise before they are fed into multi-head attentions along with decomposed queries. Interactive attentions are also presented to share vertical and horizontal contexts between rows and columns.
- We also propose efficient attentions via grouping and pooling in the feature space, which further reduces complexity to $\mathcal{O}((\beta_g + \beta_p)hw(H + W))$, with β_g and β_p the fractions of grouped and pooled features, respectively.
- Experimental results demonstrate the superior performance of DFlatFormer as a universal plug-in into various CNN and transformer backbones for semantic segmentation on multiple datasets.

2. Related work

Self-attention. For CNN based architecture, numerous efforts have been made on increasing the receptive field, through dilated convolutions or introducing self-attention modules [3, 15, 17, 18, 29]. DANet [15] employs both spatial and channel attention modules to model the semantic inter dependencies for segmentation. Traditional dense self-attention imposes heavy computation and memory cost. Various works have been proposed with improved efficiency [18, 31]. Axial self-attention [31] applies local window along horizontal and vertical axis sequentially to achieve global attention. CCNet [18] adopts self-attention on its criss-cross path in a recursive manner. These methods have shown impressive capacity in modeling long-range contextual information at a much smaller memory size and complexity.

Transformers for vision. Transformers have been known for their Superior capability in modeling long-range dependency. As a first pure transformer for vision, Vision Transformer(ViT) [13] has achieved tremendous success in image classification. Rapid and impressive progresses have been made for dense prediction [9, 12, 24, 30, 33–35, 37, 38, 41]. DETR [4] formulates the object detection into set matching problem and proposes a learnable query based framework to directly retrieve object information. MaX-DeepLab [30] employs a dual-path transformer for panoptic segmentation which contains a global memory path in addition to a

CNN path. Swin Transformer [24] employs self-attention within local windows but effectively captures long-range dependency through cyclic window shift. Pyramid vision transformer (PVT) [33] exploits hierarchical transformer structure to obtain multi-level features which greatly benefits dense prediction. SETR [41] deploys a transformer along with a simple decoder from sequence to sequence perspective. Recently SegFormer [37] presented a positional-encoding-free hierarchically structured Transformer encoder and a lightweight MLP decoder which achieves superior performance with improved computation efficiency. There is a resurgence of efficient transformer design from various aspects including attention pattern, memory, and low-rank methods [7, 21, 32].

Semantic segmentation. Since the seminal work of fully convolutional network (FCN) [25] leading to significant progress in semantic segmentation, a series of model architectures have been proposed to further improve performance. Some works target at improving the receptive field of CNNs through dilated convolution [5]. Other works improve fine-grained contexts through hierarchical structures [22, 27], exploring object contextual correlation [40], and feature refinement [20, 28]. Besides CNN-based models, Transformers [13, 21, 24, 41] have shown their capability in capturing global contexts which are important for segmentation.

3. The proposed model: DFlatFormer

In this section, we present in details the proposed Dual-Flattening transFormer (DFlatFormer). Consider a general semantic segmentation framework that consists of an encoder to extract features and a decoder for pixel-wise classification. The encoder typically gives a low-resolution feature map, and the decoder aims to output a dense feature map to enable high-resolution segmentation.

Suppose the encoder outputs a feature map $S_o \in \mathcal{R}^{h \times w \times d}$, and the decoder seeks to output a feature map $S \in \mathcal{R}^{H \times W \times d}$ at a target resolution, where $h(H)$, $w(W)$ and d are the height, width and channel dimension of encoder (decoder) feature map, respectively. Normally $h \ll H$ and $w \ll W$. Our goal is to obtain a high-resolution feature map S from the encoder output S_o through the DFlatFormer.

3.1. The overall framework

Naively, a dense transformer needs a full-size query sequence to embed a flattened sequence of low-resolution input to a high-resolution output. This is intractable as the full size sequence of $H \times W$ queries would result in demanding memory and computational overheads.

On the contrary, in the proposed DFlatFormer, we decompose full-size queries in a naive dense transformer into H row and W column ones, and use them to embed rows

and columns separately through multi-head and interactive attentions (see Sec. 3.3). The input sequence from the encoder will be flattened row-wise and column-wise to spatially align with the sequences of decomposed queries (cf. Sec. 3.2) before it is fed into row and column transformers separately. These embedded row and column representations will further interact with each other to aggregate vertical and horizontal contexts at the row-column crossing points, before they are eventually expanded and combined to generate a dense feature map of high resolution.

Fig. 1 summarizes the overall pipeline. Specially, the DFlatFormer consists of a row transformer and a column transformer. Given the low-resolution output S_o from an encoder, it is flattened row-wise and column-wise into two separate sequences R and C with the respective positional encodings (cf. Sec. 3.2). The flattened row and column sequences together with the decomposed sequences of learnable row Z_q^r and column Z_q^c queries are fed through row and column transformers to output corresponding embeddings. The resultant row/column embeddings for each layer are further refined by interacting with their column/row counterpart through an interactive attention module (see Sec. 3.3). Suppose the row (column) transformer consists of L layers, the resultant last-layer embeddings of rows Z_L^r and columns Z_L^c are finally expanded and combined to output a full-resolution feature maps S (see Sec. 3.3).

Let us take a closer look at each layer of DFlatFormer. Taking the row transformer as an example, a layer is composed of a multi-head attention (MHA) module and a row-column interactive attention module. Its MHA module takes as inputs the original row-flattened sequence R , the row query sequence Z_q^r and the last layer output of row embeddings Z_{l-1}^r , and it outputs O_l^r after a multi-layer perceptron (MLP) of Feed-Forward Network (FFN). Then a row-column interactive attention module follows by coupling intermediate embeddings of O_l^r and O_l^c output from the row and column MHAs. This module allows a row representation to aggregate all column embeddings in vertical contexts as they cross the row. It outputs the row representation of Z_l^r for layer l , which will be fed into the next layer for further modeling. The details will be presented in Sec. 3.3.

To further improve the computational efficiency, we propose a grouping and pooling module by reducing the number of row/column flattened tokens fed into each layer. The details are explained in Sec. 3.4. DFlatFormer can serve as a plug-in module to be connected to any CNN or transformer based encoder and generate high-resolution output.

3.2. Dual flattening and positional encodings

First, we flatten the encoder output S_o row-wise and column-wise to align with the row and column queries separately. This preserves the row and column structures by

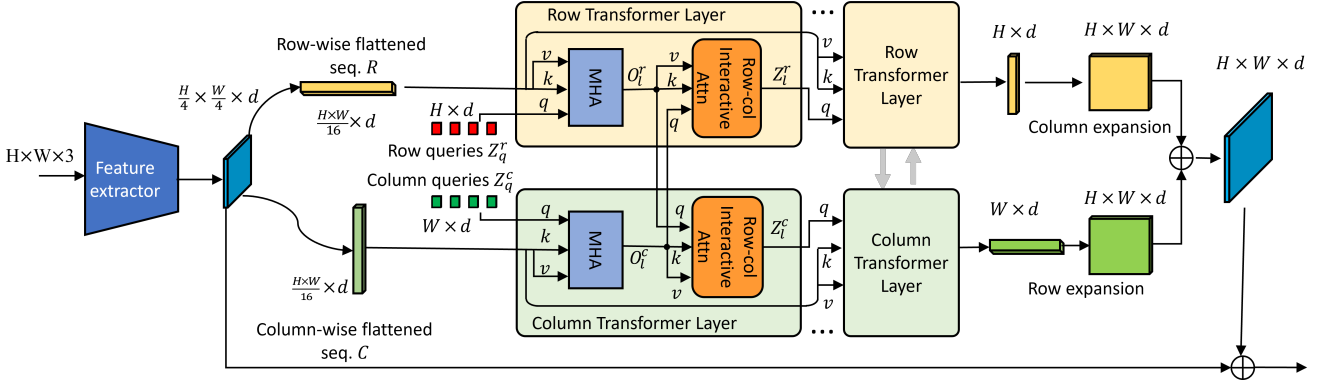


Figure 1. Illustration of DFlatFormer framework. Residual connections and normalization are omitted in the figure for better exposition to avoid unnecessary cluttering.

putting entire rows and columns together in the flattened sequences, respectively. Meanwhile, row-wise and column-wise positional encodings will also be applied to the dual-flattened sequences (cf. Sec. 3.2.1). This will enable the row and column queries to apply the multi-head attentions to the respective flattened sequences.

3.2.1 Row-wise and column-wise positional encodings

Typically, the target feature map has much larger size than the encoder output. To align the query sequence with the row/column flattened key/value sequence, we need a row/column-wise positional encodings as well.

Formally, taking the row part for example, we have a sequence of H row queries. Meanwhile, the row sequence only has h rows before it is row-wise flattened to $R \in \mathcal{R}^{h \times d}$. As shown in Fig. 2, we start with an initial 1D positional encoding $t_0^r \in \mathcal{R}^{h \times d}$ through sinusoidal function following [29]. This encoding can be upsampled by linear interpolation to $t_q^r \in \mathcal{R}^{H \times d}$, which aligns with the size of query sequence and thus can be used to initialize the positional encoding of queries directly. Meanwhile, t_0^r can also be column-wise replicated to $t_{S_0}^r \in \mathcal{R}^{h \times w \times d}$. The resultant encoding aligns with the size of input feature map S_0 , and thus can be row-wise flattened to $t_{kv}^r \in \mathcal{R}^{hw \times d}$ and used as the positional encoding of the row-wise flattened R . This is a row-wise positional encoding since each row has the same code, thereby aligning with the row-wise flattening. The similar column-wise positional encoding can be applied to the corresponding column-wise flattening.

While the above depicts the mechanism of aligning absolute positional encodings with row/column-wise flattening, it is not hard to apply the similar idea of row/column-wise expansion to extend relative positional encodings [1, 26] as well. Interested readers can refer to our source code ¹ for

more details.

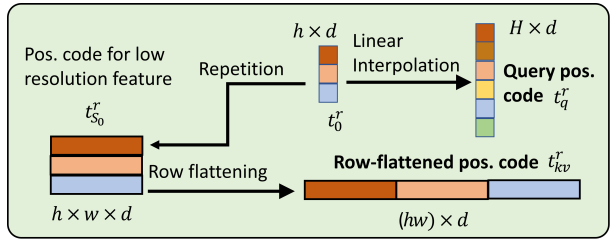


Figure 2. Positional coding of row queries and row-flattened sequence.

3.3. Multi-head and row-column interactive attentions

Multi-head attention. First we embed row and column queries separately through multi-head attention with dual-flattened sequences. Let $Z_{l-1}^r (Z_{l-1}^c)$ be the row (column) output sequence for layer $l-1$ that will be fed into the next layer as input. The first layer input $Z_0^r (Z_0^c)$ is set to 0. Then, taking a row transformer for example, a single-head attention is formulated as

$$\text{ATTN}(Z_{l-1}^r, R, Z_q^r) = Z_{l-1}^r + \text{SoftMax}\left(\frac{(Z_{l-1}^r + Z_q^r)W_q((R + t_{kv}^r)W_k)^T}{\sqrt{d_m}}\right)RW_v, \quad (1)$$

where W_q , W_k and W_v are the linear projection matrices, and d_m is the embedding dimension for each head. Z_q^r is the learnable sequence of row queries and t_{kv}^r is the positional encodings defined in Sec. 3.2.1. Then, the multi-head attention is obtained by putting together single-head outputs

$$\tilde{O}_i^r = [\text{ATTN}_0(Z_{l-1}^r, R, Z_q^r); \dots; \text{ATTN}_{n_h-1}(Z_{l-1}^r, R, Z_q^r)]W^O,$$

where W^O is a linear projection matrix. The output of each layer further goes through a feed-forward network FFN with

¹It will be available upon the acceptance of this submission.

a residual connection:

$$O_i^r = \tilde{O}_i^r + \text{FFN}(\tilde{O}_i^r).$$

Layer normalization is omitted for the notational simplicity. **Row-column interactive attention.** After a multi-head attention module, we also have a row-column interactive attention. As illustrated in Figure 3, this interactive attention aims to capture the relevant information when a row (column) crosses all columns (rows) spatially. This allows the learned row (column) representation to further integrate the vertical (horizontal) contexts along the crossed columns (rows) through an interactive attention mechanism.

Formally, the row and column outputs from their interactive attentions can be obtained below,

$$Z_i^r = \text{SoftMax}\left(\frac{O_i^r O_i^{cT}}{\sqrt{d}}\right) O_i^c + O_i^r, \quad (2)$$

$$Z_i^c = \text{SoftMax}\left(\frac{O_i^c O_i^{rT}}{\sqrt{d}}\right) O_i^r + O_i^c.$$

This module can be seen as taking the intermediate row output O_i^r as the query to aggregate the relevant information from all crossing columns. For simplicity, we do not use linear projections as in multi-head attention to map O_i^r and O_i^c into query, key and value sequences.

Final dense feature map. At the output end, each pixel at (i, j) in the final feature map is represented as a direct combination of the outputs from the row and column transformers at the same location. Formally, it can be written as

$$S_{ij} = Z_{L,i}^r + Z_{L,j}^c,$$

where S_{ij} is the final feature vector in the dense map at (i, j) , and $Z_{L,i}^r, Z_{L,j}^c$ are the representation of row i and column j in the last layer, respectively.

Note that through row-column interactive attention, each row (column) representation has already aggregated the information from all column (rows) before it is finally added to the column (row) representations to generate the dense feature output. Thus, the DFlatFormer does not wait until the final layer to re-couple rows and columns. The early interaction between rows and columns allows them to fully explore the vertical and horizontal contexts across layers while still keeping the DFlatFormer tractable.

3.4. Efficient attentions via grouping and pooling

If all the pixels in the encoder output are taken to form keys/values, the computational complexity is $\mathcal{O}(hw(H + W))$, as there are totally H rows and W columns for queries and hw keys/values fed into the DFlatFormer. To further reduce complexity, we propose to perform multi-head attention via grouping and (average) pooling. Grouping divides both queries and the input feature map into several groups,

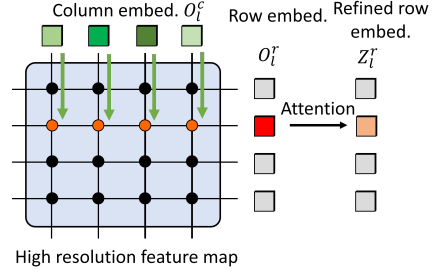


Figure 3. Illustration of row-column interactive attention, where each row(column) crosses and interacts with all columns(rows). Row-column interactive attention aims to capture these interactions to integrate information from the crossed columns (rows) to build row (column) representations.

where each query can only access features within the corresponding feature group. On the other hand, the features in a row and a column are average-pooled to form shorter flattened sequences, further reducing the model complexity.

Specifically, as shown in Fig. 4, for a row transformer, the row queries and the row-flattened sequence are equally divided into n_p groups. Multi-head attention is conducted within each group in parallel such that a row query only performs the multi-head attention on the corresponding group of the flattened sequence. On the other hand, we also average-pool the row-flattened sequence through a non-overlapping window of size n_w over each row, resulting in a shorter sequence where each row query can access the whole one for performing the multi-head attention. The resultant outputs from both grouping and pooling are added to give the output.

We note that the grouping and pooling compliment with each other – in the grouping, each query accesses a smaller but part of the flattened sequence at its original grained level. In contrast, in the pooling, the query access the whole sequence but at a coarse level with pooled features. By combining both, the output can reach a good balance between the computational cost and the representation ability.

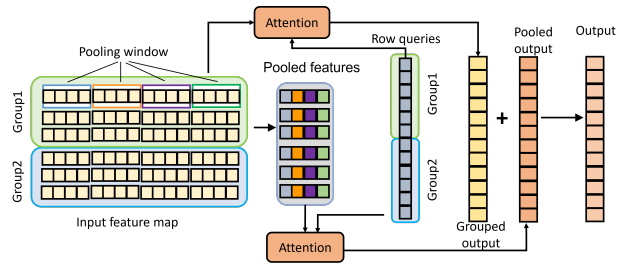


Figure 4. Attentions through grouping and pooling.

3.5. Complexity analysis

As aforementioned, with decomposed row and column queries, the overall complexity of DFlatFormer is reduced to $\mathcal{O}(hw(H + W))$. Next let us analyze the complexity with the grouping and pooling. Let $\beta_g = 1/n_p$ be the fraction of the features within each group over the flattened sequence, and $\beta_p = 1/n_w$ be the fraction of pooled features over the sequence. Each query only accesses a group of $\beta_g hw$ features. There are only $\beta_p hw$ pooled features in total, and they are shared among all the queries. Hence the total number of features that a query can access is $(\beta_g + \beta_p)hw$, resulting in an overall complexity of $\mathcal{O}((\beta_g + \beta_p)hw(H + W))$. In our experiment, we typically have $\beta_g = \frac{1}{4}$ and $\beta_p = \frac{1}{4}$, hence the overall complexity is reduced to $\mathcal{O}(\frac{1}{2}hw(H + W))$ by half.

4. Experimental results

Datasets. Experiments are conducted on three datasets: ADE20K [42], Cityscapes [11] and Pascal VOC 2012 [14]. ADE20K is a large-scale scene parsing benchmark composed of 150 classes. The number of training/validation/test images is 20k/2k/3k. Cityscapes is an urban scene understanding dataset containing 19 classes. It has 2975/500/1525 training/validation/test images. Pascal VOC consists of 21 classes, containing 1464 images with high-quality annotations, and an extra 10582 images with coarse annotations to serve as training set. The number of images for validation/testing is 1449 and 456, respectively.

Baseline and our models. With the CNN as backbone, DeepLabv3+ [5] with ResNet-50/101 are taken as the baseline models. We deploy our DFlatFormer as the decoder upon the output of DeepLabv3+ encoder. For the ResNet-50 baseline, if low-level features are explored, we implement separate DFlatFormers to take in both high-level and low-level features to generate outputs of the same spatial size. The final feature map is given by channel-wise concatenation. We present in Appendix more details of models.

Implementation details. For ADE20K and Pascal VOC datasets, we crop images into a size of 520×520 . For Cityscapes, the crop size is also 520×520 , except with MiT [37] backbone which uses 1024×1024 crop size. We adopt the standard pixel-wise cross-entropy loss as the loss function. More details are provided in Appendix.

4.1. Main results

We adopt the mean intersection over union (mIoU) to measure segmentation performance. To compare memory sizes and computation complexities, the number of parameters (“Param”) and Giga-floating-point operations (“GFLOPs”) are used. “Size” a in all tables, if not specified, denotes a crop size of $a \times a$. “mIoU” in the tables refers to mIoU with single-scale inference, and “+MS” de-

Table 1. Comparison of DFlatFormer with bilinear and DUpsample [28] on Pascal VOC *val* dataset, with backbone ResNet-50.

Scheme	w/ low-level feat.	mIoU
Bilinear		72.2
DUpsample [28]		73.2
DUpsample [28]	✓	74.2
DFlatFormer(ours)		76.7
DFlatFormer(ours)	✓	77.2

Table 2. Semantic segmentation of DFlatFormer compared with DeepLabv3+ across three datasets, with backbone ResNet-50.

Model	Pascal VOC	Cityscapes	ADE20K
DeepLabv3+ [5]	76.3	77.6	41.5
DFlatFormer(ours)	78.7 (+2.4)	79.6 (+2.0)	44.8 (+3.3)

notes mIoU with multi-scale inference and horizontal flipping.

In Table 1 we compare the DFlatFormer with ResNet-50 baseline based on bilinear upsampling and DUpsample [28]. Without low-level features, DFlatFormer gives 4.5% performance gain over bilinear upsampling and 3.5% gain over DUpsample. With exploration on low-level features, DFlatFormer provides a 0.5% additional gain in mIoU. A further comparison of DFlatFormer with PointRend [20] is given in Appendix. The above results suggest that DFlatFormer outperforms both bilinear upsampling and data-dependent upsampling in recovering high-resolution features for semantic segmentation. In Table 2 we compare performances between the DFlatFormer with DeepLabv3+ on three datasets: Pascal VOC 2012, Cityscapes and ADE20K. All methods adopt the ResNet-50 as backbone. DFlatFormer achieves 2.4%, 2.0% and 3.3% gains over DeepLabv3+ respectively. The results suggest that DFlatFormer can well capture the global contexts and achieve universal gains across datasets.

In the following we make more comparisons between our model and other state-of-art architectures, and show that the DFlatFormer can be used as a universal plug-in decoder for highly-accurate dense predictions for segmentation.

Comparison With CNN backbones. In Table 3 and Table 4, we show a comprehensive comparison of DFlatFormer with other models on ADE20K and Cityscapes *val* datasets, respectively. All models adopt the CNN backbones. For ADE20K segmentation, with ResNet-50 as backbone, DFlatFormer outperforms DeepLabv3+ baseline by 3.3% and 3.7% for single-scale and multi-scale inference, respectively; with ResNet-101 as backbone, DFlatFormer outperforms DeepLabv3+ by 2.7% for single-scale inference. For Cityscapes semantic segmentation, DFlatFormer with single-scale inference outperforms DeepLabv3+ by 2.0% and 1.8% with backbone ResNet-50 and ResNet-101, respectively.

Comparison with Transformer backbone. Given trans-

Table 3. Semantic segmentation performance on ADE20K *val* dataset with CNN backbone.

Method	Backbone	Size	Param(M)	GFLOPs	mIoU	+MS
DeepLabv3+ [5]	ResNet-50	512	43.6	176.4	41.5	43.2
MaskFormer [6]	ResNet-50	512	41	–	44.5	46.7
DFlatFormer(ours)	ResNet-50	512	45.4	407.4	44.8(+3.3)	46.9(+3.7)
Auto-DeepLab-L [23]	NAS-F48	513	–	–	44.0	–
DeepLabv3+ [5]	ResNet-101	512	62.7	255.1	43.2	44.1
CCNet [18]	ResNet-101	–	–	–	–	45.2
DANet [15]	ResNet-101	–	69	1119	45.3	–
DNL [39]	ResNet-101	–	69	1249	46.0	–
ACNet [17]	ResNet-101	–	–	–	45.9	–
SPNet [16]	ResNet-101	–	–	–	45.6	–
UperNet [36]	ResNet-101	–	86	1029	44.9	–
OCRNet [40]	ResNet-101	520	56	923	45.3	–
MaskFormer [6]	ResNet-101	512	60	–	45.5	47.2
OCRNet [40]	HRNet-w48	520	71	664	45.7	–
DFlatFormer(ours)	ResNet-101	512	68.3	512.6	45.9(+2.7)	47.2(+3.1)

former as backbone, Table 5 and Table 6 provide performance comparisons of DFlatFormer with other architectures on ADE20K *val* and Cityscapes *val* datasets, respectively. For ADE20K segmentation, with Swin-T as backbone, DFlatFormer has 2.6% gain over UperNet for single-scale inference. With Swin-S as backbone, DFlatFormer surpasses UperNet by 0.6%. On the other hand, the model size and GFLOPs of DFlatFormer are much smaller than the baselines. When comparing with SegFormer [37], with MiT-B2 as backbone, DFlatFormer outperforms SegFormer by 0.9%. With MiT-B4 as backbone, DFlatFormer outperforms SegFormer by 0.5%. While the model size is slightly increased over SegFormer, our model enjoys a much smaller GFLOPs. More detailed structure comparison with SegFormer are provided in Sec. 4.2. Note that in SegFormer, *AlignedResize* [37] is utilized which potentially provides extra gain over the normal inference. For fair comparison with others we follow the normal procedure as in MMsegmentation [10]. The results demonstrate that DFlatFormer can further leverage the multi-level features to strength the power of hierarchical structures in dense prediction.

Visualization results. For qualitative comparison, we visualize the segmentation results in Fig. 5 to compare DFlatFormer with SegFormer. It can be seen that DFlatFormer provides better predictions for small objects such as traffic signs and lights. In Fig. 6 more comparisons are presented for DeepLabv3+ (ResNet-101), SegFormer and DFlatFormer on ADE20K. From the first two images we observe that DFlatFormer can predict more accurate and complete boundaries for objects such as curtain and lamp. From the last image we observe that among the three methods, only DFlatFormer can accurately predict the segmentation for chest of drawers. The results show that DFlatFormer can effectively capture more fine-details through long-range attentions on the contexts.

Table 4. Semantic segmentation on Cityscapes *val* dataset with CNN backbone. † denotes a crop size of 512x1024.

Method	Backbone	Size	Param(M)	GFLOPs	mIoU	+MS
DeepLabv3+ [5]	ResNet-50	512	43.6	176.4	77.6	78.4
DUpsample [28]	ResNet-50	–	–	–	79.1	–
DFlatFormer(ours)	ResNet-50	512	45.4	407.4	79.6(+2.0)	80.9(+2.5)
Auto-DeepLab-L [23]	NAS-F48	769	44.4	695.0	80.3	–
DeepLabv3+ [5]	ResNet-101	512	62.7	255.1	78.8	79.3
CCNet [18]	ResNet-101	769	68.9	224.8	–	80.5
GCNet [3]	ResNet-101	–	–	–	–	78.1
DANet [15]	ResNet-101	769	–	–	–	81.5
OCRNet [40]	ResNet-101	769	–	–	–	81.8
MaskFormer [6]	ResNet-101	512†	60	–	78.5	–
DFlatFormer(ours)	ResNet-101	512	68.3	512.6	80.6(+1.8)	81.9(+2.6)

Table 5. Semantic segmentation performance on ADE20K *val* dataset, with transformer backbone. †: model pretrained on ImageNet-22K. *: *AlignedResize* used in inference.

Method	Backbone	Size	Param(M)	GFLOPs	mIoU	+MS
SETR ^T [41]	ViT-L	–	308	–	48.6	50.3
PVT+Trans2Seg	PVT-S [33]	–	32.1	31.6	42.6	–
Semantic FPN	PVT-M [33]	512	48.0	219.0	41.6	–
Semantic FPN	P2T-S [35]	512	26.8	41.7	44.4	–
Semantic FPN	P2T-B [35]	512	39.9	57.5	46.2	–
Semantic FPN	Swin-S [24]	512	53.2	270.4	45.2	–
Semantic FPN	CrossFormer-S [34]	512	34.3	220.7	46.0	–
UperNet	CrossFormer-S [34]	512	62.3	979.5	47.6	48.4
UperNet	Swin-T [24]	512	60	945	44.5	46.1
MaskFormer [6]	Swin-T	512	42	–	46.7	48.8
DFlatFormer(ours)	Swin-T	512	53.1	523.2	47.1(+2.6)	48.4(+2.3)
UperNet	Swin-S [24]	512	81.3	1038	47.6	49.3
MaskFormer [6]	Swin-S	512	63	–	49.8	51.0
DFlatFormer(ours)	Swin-S	512	72.8	719.6	48.3(+0.6)	49.8(+0.5)
Semantic FPN	CrossFormer-B [34]	512	55.6	331.0	47.7	–
Semantic FPN	CrossFormer-L [34]	512	95.4	497.0	48.7	–
UperNet	CSWin-T [12]	512	59.9	959	49.3	50.4
UperNet	CSWin-S [12]	512	64.6	1027	50.0	50.8
UperNet	Twins-SVT-B [9]	512	88.5	261	47.7	48.9
UperNet	Twins-SVT-L [9]	512	133	297	48.8	50.2
UperNet	Focal-T [38]	640	62	998	45.8	47.0
UperNet	Focal-S [38]	640	85	1130	48.0	50.0
SegFormer [37]	MiT-B2	512	27.5	62.4	46.5*	47.5
DFlatFormer(ours)	MiT-B2	512	30.5	48.4	47.4(+0.9)	48.2(+0.7)
SegFormer [37]	MiT-B4	512	64.1	95.7	50.3*	51.1
DFlatFormer(ours)	MiT-B4	512	72.7	78.4	50.8(+0.5)	51.7(+0.6)

Table 6. Semantic segmentation on Cityscapes *val* dataset with transformer backbone. ‡: crop size of 512 × 1024.

Method	Backbone	Size	Param(M)	GFLOPs	mIoU	+MS
Semantic FPN	PVT-T [33]	1024‡	17.0	–	71.7	–
Semantic FPN	P2T-T [35]	1024‡	14.9	–	77.3	–
Semantic FPN	PVT-S [33]	1024‡	28.2	–	75.5	–
Semantic FPN	P2T-S [35]	1024‡	26.8	–	78.6	–
Semantic FPN	PVT-M [33]	1024‡	48.0	–	76.6	–
Semantic FPN	P2T-B [35]	1024‡	39.9	–	79.7	–
SETR [41]	ViT	–	97.6	–	79.5	–
SETR [41]	ViT-L	–	318.3	–	82.2	–
SegFormer [37]	MiT-B2	1024	27.5	717.1	81.0	82.2
DFlatFormer(ours)	MiT-B2	1024	36.2	384.2	81.9(+0.9)	82.8(+0.6)
SegFormer [37]	MiT-B4	1024	64.1	1240.6	82.3	83.8
DFlatFormer(ours)	MiT-B4	1024	72.8	612.6	82.8(+0.5)	84.5(+0.7)

4.2. Ablation studies

Attentions through grouping and pooling. We conduct ablation study on attentions through grouping and pooling in Table 7 for ADE20K. Performance with grouping and pooling is slightly better the one without them. We hypoth-

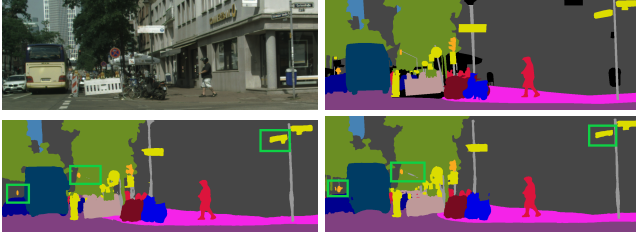


Figure 5. Cityscapes results for semantic segmentation. Top Left: RGB image; Top right: Ground-truth label; Bottom left: SegFormer; Bottom right: DFlatFormer. DFlatFormer provides better predictions for small objects such as traffic signs and lights.

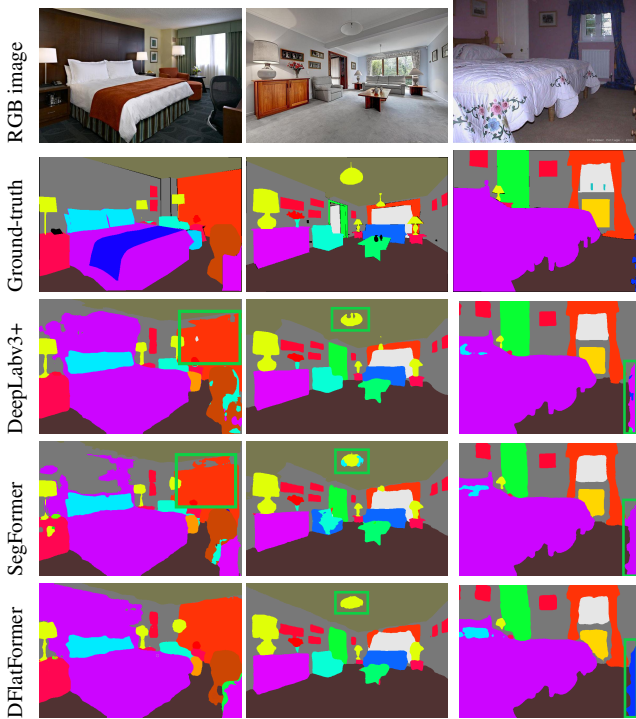


Figure 6. ADE20K segmentation examples for different schemes. DFlatFormer has better predictions than DeepLabv3+ and SegFormer for highlighted objects: first image: more complete prediction of curtain; second image: better shape prediction of lamp; third image: DFlatFormer accurately predicted chest of drawers, while other two failed.

esize that grouped features enable queries to interact more closely with spatially correlated features from neighboring rows and columns, while pooled features efficiently aggregate information from local pixels before served to model global contextual details through the DFlatFormer.

Row-column interactive attentions. We compare the performance of DFlatFormer with and without row-column interactions in Table 7 on ADE20K *val* dataset. Backbones ResNet-50 and MiT-B2 are employed. It is observed that

Table 7. DFlatFormer performance with grouping and pooling attentions, and with row-column interactive attentions.

Backbone	Grouping and pooling attentions	mIoU	
		Row-column interactions	mIoU
ResNet-50	✓	44.5	43.3
		44.8	44.8
MiT-B2	✓	47.3	46.1
		47.4	47.4

Table 8. Comparison of DFlatFormer and SegFormer with backbone MiT-B2.

Method	Performance	Decoder size and complexity	
	mIoU	Param(M)	GFLOPs
SegFormer	46.5	3.3	42.1
DFlatFormer(ours)	47.4	6.1	27.1

with interactive attentions, performance increases by 1.5% and 1.3% with backbone ResNet-50 and MiT-B2, respectively. Results demonstrate the importance of earlier interactions between rows and columns before they are eventually combined at the output end.

Comparison with SegFormer decoder. SegFormer employs a light-weighted MLP decoder with output of all-level features concatenated. Although its model size is smaller than DFlatFormer, its GFLOPs is much larger than ours. Detailed comparisons of model size and GFLOPs are presented in Table 8. We notice that an embedding dimension of 768 is employed for each hierarchical level in SegFormer to achieve decent performance. In DFlatFormer, we only set the embedding dimension up to 256. As there are four levels of output features, after the channel-wise concatenation, SegFormer has the total number of channels much larger than ours, leading to heavier computational cost as well as memory footprint although it has a smaller number of model parameters.

Ablations on other factors. The comparisons of other factors are presented in Appendix, including positional codes and number of decoder layers, etc.

5. Conclusion

We propose a dual-flattening transformer to learn dense feature maps for high-resolution semantic segmentation. Given an input feature map of size $h \times w$ and an output target of size $H \times W$, the proposed model merely incurs a complexity of $\mathcal{O}(hw(H+W))$ by employing decomposed row and column queries to capture global attentions. Input feature maps are row-wise and column-wise flattened to maintain their row and column structures, and hence the decomposed queries can retrieve immediate contexts from neighboring rows and columns. To recover the spatial details of high resolution, we introduce row-column interactive attentions at their crossing points. We further present

efficient attentions via grouping and pooling in the feature space to further reduce the complexity. Experiments have demonstrated superior performances of the proposed DFlatFormer over others with both CNN and Transformer backbones.

References

- [1] Irwan Bello, Barret Zoph, Ashish Vaswani, Jonathon Shlens, and Quoc V Le. Attention augmented convolutional networks. In *Proceedings of the IEEE/CVF international conference on computer vision*, pages 3286–3295, 2019. 4
- [2] Iz Beltagy, Matthew E Peters, and Arman Cohan. Longformer: The long-document transformer. *arXiv preprint arXiv:2004.05150*, 2020. 2
- [3] Yue Cao, Jiarui Xu, Stephen Lin, Fangyun Wei, and Han Hu. Gcnet: Non-local networks meet squeeze-excitation networks and beyond. In *Proceedings of the IEEE/CVF International Conference on Computer Vision Workshops*, pages 0–0, 2019. 1, 2, 7
- [4] Nicolas Carion, Francisco Massa, Gabriel Synnaeve, Nicolas Usunier, Alexander Kirillov, and Sergey Zagoruyko. End-to-end object detection with transformers. In *European Conference on Computer Vision*, pages 213–229. Springer, 2020. 2
- [5] Liang-Chieh Chen, Yukun Zhu, George Papandreou, Florian Schroff, and Hartwig Adam. Encoder-decoder with atrous separable convolution for semantic image segmentation. In *Proceedings of the European conference on computer vision (ECCV)*, pages 801–818, 2018. 3, 6, 7
- [6] Bowen Cheng, Alexander G Schwing, and Alexander Kirillov. Per-pixel classification is not all you need for semantic segmentation. *arXiv preprint arXiv:2107.06278*, 2021. 7
- [7] Rewon Child, Scott Gray, Alec Radford, and Ilya Sutskever. Generating long sequences with sparse transformers. *arXiv preprint arXiv:1904.10509*, 2019. 3
- [8] François Chollet. Xception: Deep learning with depthwise separable convolutions. In *Proceedings of the IEEE conference on computer vision and pattern recognition*, pages 1251–1258, 2017. 2
- [9] Xiangxiang Chu, Zhi Tian, Yuqing Wang, Bo Zhang, Haibing Ren, Xiaolin Wei, Huaxia Xia, and Chunhua Shen. Twins: Revisiting the design of spatial attention in vision transformers. *arXiv preprint arXiv:2104.13840*, 1(2):3, 2021. 2, 7
- [10] MMSegmentation Contributors. MMSegmentation: Openmmlab semantic segmentation toolbox and benchmark. <https://github.com/open-mmlab/mms Segmentation>, 2020. 7
- [11] Marius Cordts, Mohamed Omran, Sebastian Ramos, Timo Rehfeld, Markus Enzweiler, Rodrigo Benenson, Uwe Franke, Stefan Roth, and Bernt Schiele. The cityscapes dataset for semantic urban scene understanding. In *Proceedings of the IEEE conference on computer vision and pattern recognition*, pages 3213–3223, 2016. 6
- [12] Xiaoyi Dong, Jianmin Bao, Dongdong Chen, Weiming Zhang, Nenghai Yu, Lu Yuan, Dong Chen, and Baining Guo. Cswin transformer: A general vision transformer backbone with cross-shaped windows. *arXiv preprint arXiv:2107.00652*, 2021. 2, 7
- [13] Alexey Dosovitskiy, Lucas Beyer, Alexander Kolesnikov, Dirk Weissenborn, Xiaohua Zhai, Thomas Unterthiner, Mostafa Dehghani, Matthias Minderer, Georg Heigold, Sylvain Gelly, et al. An image is worth 16x16 words: Transformers for image recognition at scale. In *International Conference on Learning Representations*, 2020. 1, 2, 3
- [14] Mark Everingham, Luc Van Gool, Christopher KI Williams, John Winn, and Andrew Zisserman. The pascal visual object classes (voc) challenge. *International journal of computer vision*, 88(2):303–338, 2010. 6
- [15] Jun Fu, Jing Liu, Haijie Tian, Yong Li, Yongjun Bao, Zhiwei Fang, and Hanqing Lu. Dual attention network for scene segmentation. In *Proceedings of the IEEE/CVF Conference on Computer Vision and Pattern Recognition*, pages 3146–3154, 2019. 2, 7
- [16] Qibin Hou, Li Zhang, Ming-Ming Cheng, and Jiashi Feng. Strip pooling: Rethinking spatial pooling for scene parsing. In *Proceedings of the IEEE/CVF Conference on Computer Vision and Pattern Recognition*, pages 4003–4012, 2020. 7
- [17] Xinxin Hu, Kailun Yang, Lei Fei, and Kaiwei Wang. Acnet: Attention based network to exploit complementary features for rgbd semantic segmentation. In *2019 IEEE International Conference on Image Processing (ICIP)*, pages 1440–1444. IEEE, 2019. 1, 2, 7
- [18] Zilong Huang, Xinggang Wang, Lichao Huang, Chang Huang, Yunchao Wei, and Wenyu Liu. CCNet: Criss-cross attention for semantic segmentation. In *Proceedings of the IEEE/CVF International Conference on Computer Vision*, pages 603–612, 2019. 1, 2, 7
- [19] Alexander Kirillov, Ross Girshick, Kaiming He, and Piotr Dollár. Panoptic feature pyramid networks. In *Proceedings of the IEEE/CVF Conference on Computer Vision and Pattern Recognition*, pages 6399–6408, 2019. 7
- [20] Alexander Kirillov, Yuxin Wu, Kaiming He, and Ross Girshick. Pointrend: Image segmentation as rendering. In *Proceedings of the IEEE/CVF conference on computer vision and pattern recognition*, pages 9799–9808, 2020. 1, 3, 6
- [21] Nikita Kitaev, Lukasz Kaiser, and Anselm Levskaya. Reformer: The efficient transformer. In *International Conference on Learning Representations*, 2019. 3
- [22] Tsung-Yi Lin, Piotr Dollár, Ross Girshick, Kaiming He, Bharath Hariharan, and Serge Belongie. Feature pyramid networks for object detection. In *Proceedings of the IEEE conference on computer vision and pattern recognition*, pages 2117–2125, 2017. 3
- [23] Chenxi Liu, Liang-Chieh Chen, Florian Schroff, Hartwig Adam, Wei Hua, Alan L Yuille, and Li Fei-Fei. Auto-deeplab: Hierarchical neural architecture search for semantic image segmentation. In *Proceedings of the IEEE/CVF Conference on Computer Vision and Pattern Recognition*, pages 82–92, 2019. 7
- [24] Ze Liu, Yutong Lin, Yue Cao, Han Hu, Yixuan Wei, Zheng Zhang, Stephen Lin, and Baining Guo. Swin transformer: Hierarchical vision transformer using shifted windows. *arXiv preprint arXiv:2103.14030*, 2021. 1, 2, 3, 7

- [25] Jonathan Long, Evan Shelhamer, and Trevor Darrell. Fully convolutional networks for semantic segmentation. In *Proceedings of the IEEE conference on computer vision and pattern recognition*, pages 3431–3440, 2015. 3
- [26] Peter Shaw, Jakob Uszkoreit, and Ashish Vaswani. Self-attention with relative position representations. *arXiv preprint arXiv:1803.02155*, 2018. 4
- [27] Andrew Tao, Karan Sapra, and Bryan Catanzaro. Hierarchical multi-scale attention for semantic segmentation. *arXiv preprint arXiv:2005.10821*, 2020. 3
- [28] Zhi Tian, Tong He, Chunhua Shen, and Youliang Yan. Decoders matter for semantic segmentation: Data-dependent decoding enables flexible feature aggregation. In *Proceedings of the IEEE/CVF Conference on Computer Vision and Pattern Recognition*, pages 3126–3135, 2019. 1, 3, 6, 7
- [29] Ashish Vaswani, Noam Shazeer, Niki Parmar, Jakob Uszkoreit, Llion Jones, Aidan N Gomez, Łukasz Kaiser, and Illia Polosukhin. Attention is all you need. In *Advances in neural information processing systems*, pages 5998–6008, 2017. 2, 4
- [30] Huiyu Wang, Yukun Zhu, Hartwig Adam, Alan Yuille, and Liang-Chieh Chen. Max-deeplab: End-to-end panoptic segmentation with mask transformers. In *Proceedings of the IEEE/CVF Conference on Computer Vision and Pattern Recognition*, pages 5463–5474, 2021. 2
- [31] Huiyu Wang, Yukun Zhu, Bradley Green, Hartwig Adam, Alan Yuille, and Liang-Chieh Chen. Axial-deeplab: Stand-alone axial-attention for panoptic segmentation. In *European Conference on Computer Vision*, pages 108–126. Springer, 2020. 1, 2
- [32] Sinong Wang, Belinda Z Li, Madian Khabsa, Han Fang, and Hao Ma. Linformer: Self-attention with linear complexity. *arXiv preprint arXiv:2006.04768*, 2020. 3
- [33] Wenhai Wang, Enze Xie, Xiang Li, Deng-Ping Fan, Kaitao Song, Ding Liang, Tong Lu, Ping Luo, and Ling Shao. Pyramid vision transformer: A versatile backbone for dense prediction without convolutions. *arXiv preprint arXiv:2102.12122*, 2021. 1, 2, 3, 7
- [34] Wenxiao Wang, Lu Yao, Long Chen, Deng Cai, Xiaofei He, and Wei Liu. Crossformer: A versatile vision transformer based on cross-scale attention. *arXiv preprint arXiv:2108.00154*, 2021. 2, 7
- [35] Yu-Huan Wu, Yun Liu, Xin Zhan, and Ming-Ming Cheng. P2T: Pyramid pooling transformer for scene understanding. *arXiv preprint arXiv:2106.12011*, 2021. 1, 2, 7
- [36] Tete Xiao, Yingcheng Liu, Bolei Zhou, Yuning Jiang, and Jian Sun. Unified perceptual parsing for scene understanding. In *Proceedings of the European Conference on Computer Vision (ECCV)*, pages 418–434, 2018. 7
- [37] Enze Xie, Wenhai Wang, Zhiding Yu, Anima Anandkumar, Jose M Alvarez, and Ping Luo. Segformer: Simple and efficient design for semantic segmentation with transformers. *arXiv preprint arXiv:2105.15203*, 2021. 1, 2, 3, 6, 7
- [38] Jianwei Yang, Chunyuan Li, Pengchuan Zhang, Xiyang Dai, Bin Xiao, Lu Yuan, and Jianfeng Gao. Focal self-attention for local-global interactions in vision transformers. *arXiv preprint arXiv:2107.00641*, 2021. 2, 7
- [39] Minghao Yin, Zhuliang Yao, Yue Cao, Xiu Li, Zheng Zhang, Stephen Lin, and Han Hu. Disentangled non-local neural networks. In *European Conference on Computer Vision*, pages 191–207. Springer, 2020. 7
- [40] Yuhui Yuan, Xilin Chen, and Jingdong Wang. Object-contextual representations for semantic segmentation. In *Computer Vision–ECCV 2020: 16th European Conference, Glasgow, UK, August 23–28, 2020, Proceedings, Part VI 16*, pages 173–190. Springer, 2020. 3, 7
- [41] Sixiao Zheng, Jiachen Lu, Hengshuang Zhao, Xiatian Zhu, Zekun Luo, Yabiao Wang, Yanwei Fu, Jianfeng Feng, Tao Xiang, Philip HS Torr, et al. Rethinking semantic segmentation from a sequence-to-sequence perspective with transformers. In *Proceedings of the IEEE/CVF Conference on Computer Vision and Pattern Recognition*, pages 6881–6890, 2021. 2, 3, 7
- [42] Bolei Zhou, Hang Zhao, Xavier Puig, Sanja Fidler, Adela Barriuso, and Antonio Torralba. Scene parsing through ADE20K dataset. In *Proceedings of the IEEE conference on computer vision and pattern recognition*, pages 633–641, 2017. 6